A NIR spectrometer onboard Uvsq-Sat NG satellite for observing greenhouse gases

Cannelle Clavier, Mustapha Meftah, Nicolas Rouanet, Jean-François Mariscal

A NIR Spectrometer Onboard Uvsq-Sat NG satellite for Observing Greenhouse Gases

Cannelle Clavier[a,b], Mustapha Meftah[a], Nicolas Rouanet[a], and Jean-François Mariscal[a]

[a]Université de Versailles Saint-Quentin-en-Yvelines, Université Paris-Saclay, Sorbonne Université (SU), LATMOS, 11 Boulevard d'Alembert, 78280 Guyancourt, France
[b]ACRI-ST – CERGA, 10 Avenue Nicolas Copernic, 06130 Grasse, France

ABSTRACT

Uvsq-Sat NG is a Six-Unit GHG CubeSat dedicated to the simultaneous measurements of the Earth Radiation Budget and greenhouse gases. This space mission aims to evaluate the potential of using a compact spectrometer mounted on a CubeSat for determining atmospheric GHG concentrations (CO_2, CH_4). This spectrometer operates in the Near-Infrared (NIR) range, typically between 1200 to 2000 nm, which is an ideal wavelength range for detecting and measuring the spectral signatures of the most significant greenhouse gases. The inclusion of such a spectrometer on Uvsq-Sat NG represents an important step forward in climate research. It not only provides essential data for environmental science but also demonstrates the growing capability of satellite technology to support crucial observations of our planet's changing climate. The aim of this article is to present an optical configuration for this instrument. The performance achieved with this design will be presented. We will see if the proposed instrument design is capable of measuring greenhouse gas concentrations with good accuracy (absolute measurements of ±4.0 ppm with an annual stability of ±1.0 ppm for CO_2, absolute measurements of ±25.0 ppb with an annual stability of ±10.0 ppb for CH_4).

Keywords: Uvsq-Sat NG, Satellite, Spectrometer, Greenhouse Gases, Near-Infrared

1. INTRODUCTION

Climate change is one the main issue of the 21^{st} century. The increase in extreme weather events, rising sea levels and rising global temperatures of the Earth will have non negligible consequences on societies. The 5^{th} IPCC report forecasts an Earth's temperature rise up to 4.8° by 2100 (1). To avoid the worst-case climate scenarios, global and national governments have introduced precautionary measures to attenuate the effects of climate change. In 2015, 195 countries pledged to reduce their Greenhouse Gas (GHG) emissions at the Paris conference during the Conference Of the Parties 21 (COP21). The objective was to maintain a temperature rise of less than 1.5°C compared to the Earth's average temperature before the pre-industrial era (2). In 2024, the Earth's average temperature almost reached 1.5°C and GHG concentrations have continued to increase. GHG concentrations are one of the significant Essential Climate Variables (ECV) that contribute the most to the global warming trend. It is of paramount importance to develop observation tools that can quantify the sources and sinks of greenhouse gas emissions at the local scale and in near-real time. These data are essential for the study of carbon and methane cycles on short time scales, as well as for the implementation of public policies aimed at reducing greenhouse gas emissions. For these purposes, space-based instruments are key assets for global monitoring of the CO_2 and CH_4 columns. Anthropogenic emissions of these two gases are the major contributors to global warming. Their monitoring all over the globe must be devised with excellent spatial and temporal resolutions. To extend the revisit time of a single space-based instrument, a constellation of satellites may be considered.

CubeSats are the preferred choice for rapid development of operational instruments and satellite constellations for near-real time monitoring. A CubeSats constellation at a Low Earth Orbit (LEO) has the advantage to monitor the entire globe while the satellites on Geostationnary Orbit (GEO) can't see the polar regions which

Further author information: (Send correspondence to C. Clavier)
C. Clavier: E-mail: cannelle.clavier@latmos.ipsl.fr

are regions of interest to study the permafrost according to the rapid evolution of global warming (3). Moreover, thanks to their distance from Earth, the CubeSats at LEO can have better spatial resolution when they take a narrow field of view instrument onboard. However, a constellation of CubeSats designed for near-real-time monitoring requires the deployment of a greater number of satellites and the use of miniaturized instruments. Consequently, the instruments traditionally carried on large satellites must be miniaturized. This represents a significant challenge for the space industry in the 21^{st} century. To determine CO_2 and CH_4 concentrations from a CubeSat, a NIR spectrometer is a good candidate to that purpose. Despite its miniaturization, the spectrometer must maintain performance levels relevant for climate research. To demonstrate that it is possible to measure GHG accurately using a miniaturized spectrometer, the Laboratoire Atmosphères, Observations Spatiales (LATMOS) is developing an innovative CubeSat. Uvsq-Sat NG is a French nanosatellite whose mission is to demonstrate the SmallSat relevance to initiate a constellation of satellites for CO_2 and CH_4 concentrations monitoring. To identify the sources and the sinks of GHG emissions, the Global Climate Observing System (GCOS) (4) requires that the CO_2 and the CH_4 measurements must be made with an absolute accuracy of ± 0.6 ppm and ± 7 ppb. For good repeatability over time, the stability per decade required is ± 0.1 ppm for CO_2 measurements and ± 1 ppb for CH_4 measurements. All the GCOS scientific requirements are listed in Table 1. As a pathfinder, the Uvsq-Sat NG's objective is to demonstrate that a SmallSat with a miniaturized instrument will be able to detect CO_2 and CH_4 with an absolute accuracy of ± 4.0 ppm and ± 25.0 ppb and a annual stability of ± 1.0 ppm for the CO_2 and ± 10.0 ppb for the CH_4 (5). This Six-Unit CubeSat can carry a payload of One-Unit, i.e. a spectrometer no larger than 10 cm. The method used to determine GHG concentrations from the Uvsq-Sat NG spectrometer has been detailed in Meftah et al. 2023 (5). To fulfill the scientific requirements, a low-resolution spectrometer must satisfy excellent radiometric performances, which is challenging for a miniaturized instrument.

CO_2 scientific requirements			
Absolute accuracy (2σ)	**Stability per decade**	**Spatial resolution**	**Temporal resolution**
$\pm$ 0.6 ppm	$\pm$ 0.1 ppm	0.3 km	1 h
CH_4 scientific requirements			
Absolute accuracy (2σ)	**Stability per decade**	**Spatial resolution**	**Temporal resolution**
$\pm$ 7 ppb	$\pm$ 7 ppb	0.3 km	1 h

Table 1: Global Climate Observing System scientific requirements for GHG observations.

The purpose of this paper is to present an optical design of a miniaturized spectrometer that could be used onboard Uvsq-Sat NG. Section 2 details the technical requirements for the miniaturized spectrometer and the method used to select an optical design. Section 3 analyzes the optical performances of the spectrometer and determines the main optical characteristics such as the spectral resolution and the slit functions. Section 4 presents the radiometric performances of the spectrometer according to simulated spectral irradiances at the Top Of the Atmosphere (TOA). The instrument design must fulfill the optical and radiometric performances to be able to achieve the scientific mission according to the scientific requirements. Finally, Section 5 outlines a methodology for the design of a future instrument with higher spectral resolution ($\sim$1 nm). The instrument would enable more acurate detection of GHG sources and sinks, while meeting the measurement requirements of the GCOS.

2. DESCRIPTION OF THE UVSQ-SAT NG'S PAYLOAD

The Uvsq-Sat NG spectrometer is a pathfinder designed to demonstrate the value of miniaturised instrument onboard SmallSat for GHG monitoring. The satellite is scheduled for launch in 2025 and will inaugurate a CubeSat constellation for near-real time Earth observation. The objective here is to present the designed miniaturized spectrometer similar to the one onboard Uvsq-Sat NG. This forerunner instrument must be able to determine GHG over a maximum of daylight observation scenes at a local scale. The CO_2 must be determined with a ± 4.0 ppm accuracy and the CH_4 with a ± 25.0 ppb accuracy.

The main difficulty in designing a miniaturized instrument is to achieve measurement performances similar to that of non-miniaturized ones. In order to meet the scientific measurement requirements, the designed spectrom-

eter must satisfy some technical requirements described in Meftah et al. 2023 (5). All the essential requirements for the design of the Uvqs-Sat NG spectrometer are listed below and are summarized in Table 2:

Uvsq-Sat NG Spectrometer	
Spectrometer volume	1 Unit (10×10×10 cm^3)
Spectral range	1200 - 2000 nm
Spectral resolution	<6 nm
SNR	>500
Sensor	Linear sensor of 256 pixels
Pixels size	50 × 250 µm
Field of view	0.15°

Table 2: Technical requirements of the Uvsq-Sat NG spectrometer

- Spectrometer's size: Uvsq-Sat NG can carry a One-Unit payload for GHG observation. This implies that the volume of the spectrometer must be integrated in a 10 cm cube. The optical design described in this paper must considered the space needed for the mechanical design and for assembly of the components. To satisfy the size requirements, the number of optical elements must be reduce to a minimum of elements. This is the most difficult part of designing a spectrometer for CubeSat given the scientific requirements.

- Spectral requirements: To determine the GHG concentrations, Uvsq-Sat NG uses the Levenberg-Marquardt method, which requires a continuous spectrum in the 1200-2000 nm range. Considering the size of the spectrometer and the need to measure a spectrum over the extended range from 1200 to 2000 nm, the design spectrometer is a single-grating spectrometer inspired by an Ebert-Fastie configuration. However, the design of a miniaturized grating spectrometer will limit spectral resolution to a few nanometers for a spectral range of 800 nm. For the Uvsq-Sat NG spectrometer, the expected spectral resolution of the spectrometer must be better than 6 nm.

- Radiometric requirements: With a low-resolution spectrometer, the Signal to Noise Ratio (SNR) must be excellent to meet the scientific requirements. The minimum SNR required is 500 for a 6 nm spectral resolution, while for a 1 nm spectrometer, a minimum SNR of 250 is necessary. The 1200-2000 nm measured spectrum is the result of the Sun's radiative transfer in the atmosphere. The measurement thus depends on the specific observation scene. The incoming irradiance varies depending on the surface observed and the solar and atmospheric conditions. For a nadir pointed satellite, the two extreme scenarios of observation are measurements above oceans, where the signal is low, and above the polar regions, where the solar irradiance is highly reflected by the ice (6). The spectrometer must meet the radiometric requirements for all these scenarios. The signal must be sufficiently high to meet the specified SNR requirements without exceeding the saturation level of the sensor.

- Sensor: To operate in the 1200-2000 nm range, we choose a Complementary Metal-Oxide-Semiconductor (CMOS) sensor made of Indium Gallium Arsenide (InGaAs). For the thermal stability, the sensor is cooled with a Peltier thermoelectric cooler. The measurements are susceptible to fluctuations in the sensor's temperature due to the influence of the dark current, which is dependent on the surrounding temperature. Therefore, it is essential to maintain a stable temperature for optimal sensor performance. The selected sensor is a linear image sensor of 256 pixels measuring 0.25 × 12.8 mm^2. Each pixel measures 250 × 50 μm^2 and have an active area of 250 × 30 μm^2. This sensor has been selected due to its low noise and low dark current characteristics.

- Field of view and spatial resolution: To identify GHG sources and sinks at local scale, the spatial resolution of the spectrometer can't exceed few km on the ground. Uvsq-Sat NG will be launched on a LEO at 600 km of altitude. Therefore, to minimize the spatial resolution, the field of view chosen for the Uvsq-Sat NG spectrometer design is 0.15°, which represent a ground footprint of less than 2 km. As the spectrometer is not a spectro-imager, the instrument's field of view and spatial resolution are intrinsically linked.

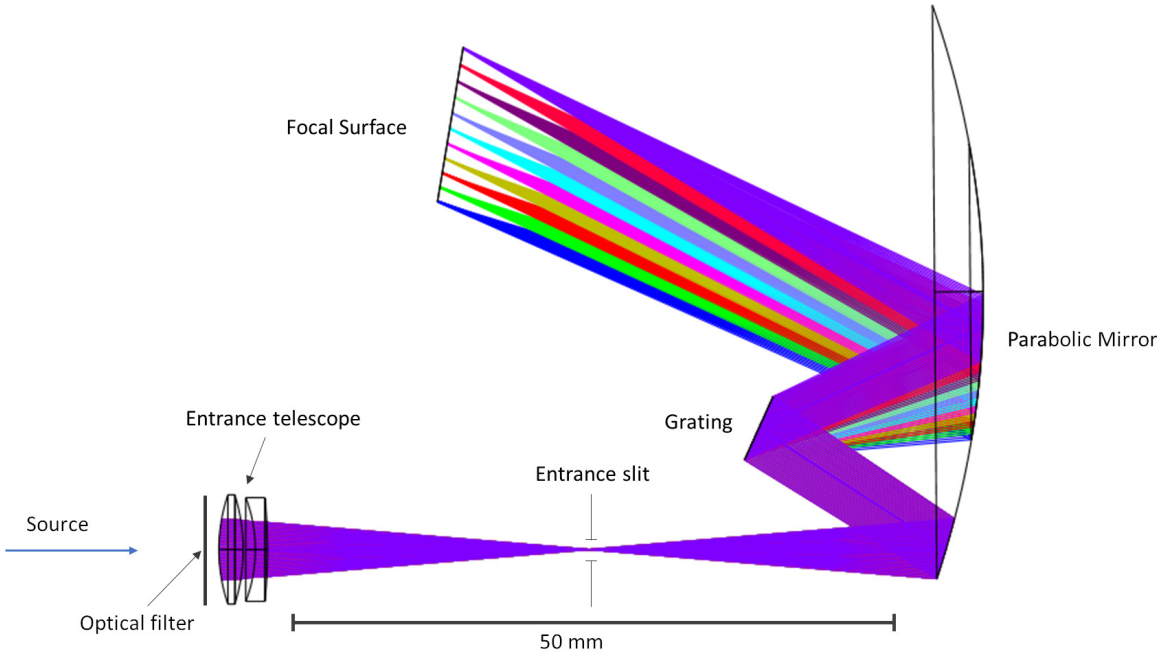

Figure 1: Optical layout.

The optical design of the miniaturized spectrometer has been built with the Zemax OpticStudio software. The optimization of the system has been made thanks to the requirements defined above. Figure 1 illustrates the optical design of the miniaturized spectrometer.

The dimensions of the whole optical system match with an integration in an One-Unit payload. First of all, the entrance of the spectrometer is defined by an entrance telescope, which has a circular aperture of 5 mm and a 30 mm focal lens. The entrance telescope is composed of two lenses, each made of a different type of glass. One is made of CaF_2, while the other is made of Infrasil. This doublet focus the light on the entrance slit with a negligible spot size in comparison to the slit size. The dimensions of the entrance slit influence the spectral resolution, field of view, and radiometric performance of the instrument. A narrow slit enhances spectral resolution and minimizes the ground footprint, but it also decreases the spectrometer's radiometric performance. The choice of entrance slit size is crucial for measuring GHG concentrations with good accuracy. In the following analyses, the slit width is 50 µm. Then the light is collimated by a parabolic mirror on a diffraction grating (300 groves per mm) that is used at first diffraction order. To prevent spectrum aliasing on the sensor for wavelengths outside the 1200-2000 nm range, an optical filter is added to the spectrometer entrance, transmitting only the wavelength band of interest. Finally, the light scattered by the grating is focused on the sensor by the parabolic mirror.

This section presents an optical design, which meets the dimensions requirements. The following optical and radiometric analyses determine whether or not this optical design can meet the technical requirements for the Uvsq-Sat NG mission. The analysis below does not consider stray light, but a study is needed to fully qualify the performance of such an instrument. In particular, the 0 order of the grating could have an impact on the resolution and radiometric performance. Such a study will allow the design of a mechanical architecture to reduce the impact of stray light, for example by adding optical baffles.

3. OPTICAL PERFORMANCES OF THE SPECTROMETER

Miniaturizing an instrument can severely damaged its performances and hence the GHG measurements accuracy. To evaluate the optical performance of an instrument, the characteristic parameter to be analyzed is the Point

Spread Function (PSF). In the case of the Uvsq-Sat NG spectrometer, the PSF is defined as the instrument's response to the 50 µm entrance slit for a given monochromatic wave.

Spectral resolution is the most important parameter to analyze to validate the spectrometer's optical performances. However, other parameters must be examined, such as the PSF's shape on the sensor, or the linearity of the dispersion on the sensor. In this Section, we analyse the spectral resolution of the spectrometer based on two optical results: the Full Width at Half Maximum (FWHM) and the Root Mean Square (RMS) of each PSF. Both analyses validate the spectrometer's optical performances, and specifically if its spectral resolution is less than 6 nm over the entire 1200-2000 nm range. The FWHM is a typical physical quantity used to qualify the spectral resolution. However, this definition of spectral resolution has limitations, the study of the RMS is complementary to that of the FWHM and allows a better qualification of the spectral response of the instrument.

To study the FWHM and the RMS, the Zemax OpticStudio software launches random rays with a 0.15° field of view to fully and uniformly illuminate the entrance slit. The software then counts the rays at different positions on the sensor. The value obtained represents a power with an arbitrary unit on the sensor before detection. For RMS and FWHM calculations, the powers of the peaks have been normalized.

3.1 Spectral Resolution Based on the Full Width at Half Maximum Criterion

The spectral resolution of a spectrometer is usual expressed using the FWHM. Equation 1 defines the $FWHM_{PSF}$ function on the sensor for each monochromatic wave. For a normalized PSF on the sensor, the $FWHM_{PSF}$ represents the distance between the two positions where the power of the normalized PSF is equal to 0.5. For high resolution, the energy spread must be concentrated on a point of the sensor. In the Uvsq-Sat NG's case, the 1200-2000 nm must be scattered on a 12.8 mm sensor. So to reach a maximum of 6 nm resolution, the energy spread of a monochromatic wave should be less than 96 µm, which represents less than two pixels.

$$FWHM_{PSF} = |x_{P_{1,PSF}} - x_{P_{2,PSF}}| \tag{1}$$

where $x_{P_{PSF}}$ are the two positions on the sensor where the monochromatic wave λ has a contribution of half of the position where the contribution of the wave is maximum. For illustration, Figure 2 represents the $FWHM_{PSF}$ at 1200 nm. The profiles shown also highlight the non-Gaussian shape of the PSF.

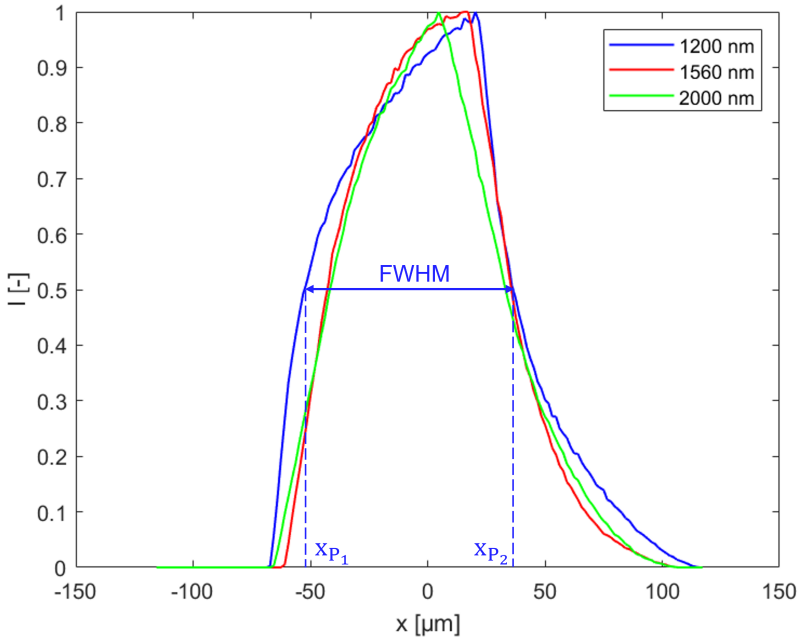

Figure 2: PSF's profiles on the sensor and $FWHM_{PSF}$ at 1200 nm.

To determine the $FWHM_{PSF}$ over the entire 1200-2000 nm spectrum, we analyzed 21 monochromatic waves distributed between 1200 and 2000 nm with a 40 nm step. From Zemax OpticStudio image spots, the dimension of the 21 $FWHM_{PSF}$ could be evaluated. Equation 2 describes the relation between the $FWHM_{PSF}$ on the sensor and the spectral $FWHM_{\lambda}$. This equation is used to switch from the spatial domain of the sensor to the spectral domain.

$$\frac{FWHM_{\lambda}}{\Delta\lambda} = \frac{FWHM_{PSF}}{\Delta x} \tag{2}$$

where $FWHM_{\lambda}$ is the spectral FWHM, $\Delta\lambda$ is spectral range between 1200 and 2000 nm, $FWHM_{PSF}$ is the FWHM on the sensor and Δx is the sensor's size.

Figure 3 shows the spectral resolution of the designed Uvsq-Sat NG spectrometer based on a $FWHM_{\lambda}$ criterion. Results show compliance with technical requirements for spectral resolution. Furthermore, the study shows that a grating alignment error of 0.2° has no impact on the spectral resolution of the spectrometer. The optical alignments of this miniaturized instrument can be tricky, so studying the instrument's sensitivities to optical element alignments is fundamental to validating the instrument's performances.

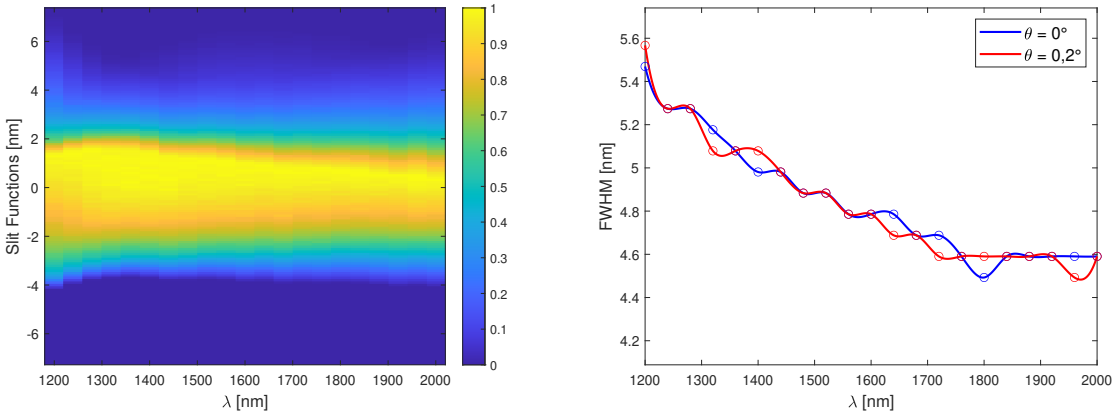

Figure 3: Slit functions of the Uvsq-Sat NG spectrometer for 21 monochromatic waves between 1200 and 2000 nm (left) and $FWHM_{\lambda}$ for each wavelength in the case where the grating is perfectly aligned according to the optical layout and in the case where the grating is misaligned by 0.2° compared to the nominal optical layout (right).

3.2 Spectral Resolution Based on the Root Mean Square Criterion

The FWHM criterion for evaluating the spectral resolution of a spectrometer provides only partial information about the PSF. For instance, it does not consider the total spread of the PSF on the sensor. This is the validation criterion commonly used to describe the spectral resolution of an instrument, however a PSF could meet the FWHM criterion while being largely spread on the sensor, potentially impinging on neighboring pixels. It is typically used for PSF with gaussian shapes but Figure 2 clearly shows that the PSF are not gaussian. The PSF spreads out strongly on one of its sides, so some of its energy can be detected by many pixels. To complete the precedent study, we analyzed the PSF's RMS, which represents the PSF's spread weighted by the intensity on each point on the sensor. Equation 3 describes the definition used to calculate the PSF's RMS. This study can be used to determine whether the overall spread of the PSF is too great on the sensor. The validation criterion based on the FWHM could be met, whereas the one based on the RMS could not. For two equal FWHMs, the flux distribution on the sensor can be different. The two studies are complementary.

$$\sigma_{RMS,\lambda} = \sqrt{\frac{\sum_i (x_i - \bar{x_{\lambda}})^2 \times P_{\lambda,i}}{\sum_j P_{\lambda,j}}} \tag{3}$$

where $\sigma_{RMS,\lambda}$ is the RMS of the PSF, $P_{\lambda,i}$ is the normalized flux contribution of the monochromatic wave λ on the sensor's position x_i and $\bar{x_\lambda}$ is the barycenter of the flux contributions of λ on the sensor. The barycenter is calculated as below:

$$\bar{x_\lambda} = \frac{\sum_i P_{\lambda,i} \times x_i}{\sum_j P_{\lambda,j}}$$

To analyze the PSF's RMS and their impact on the optical performances of the Uvsq-Sat NG spectrometer, we need a validation criterion. Equation 4 defines a validation criterion in the case where the PSF are Gaussian, which is not the case with the Uvsq-Sat NG spectrometer. However, for a preliminary approximation, it enables the establishment of a validation criterion based on $\sigma_{RMS,\lambda}$. Based on Equation 2, $\sigma_{RMS,\lambda}$ can't exceed 41 µm.

$$\sigma_{RMS,\lambda} = \frac{FWHM_\lambda}{2\sqrt{2ln(2)}} \tag{4}$$

Figure 4 shows the RMS for the 21 analyzed waves. The results show that the designed spectrometer meets the performances criteria based on the PSF's RMS to get a 6 nm resolution spectrometer. However, the RMS is not constant on all 1200-2000 nm range, which means that PSF's profiles have undergoes various modifications through the optical system.

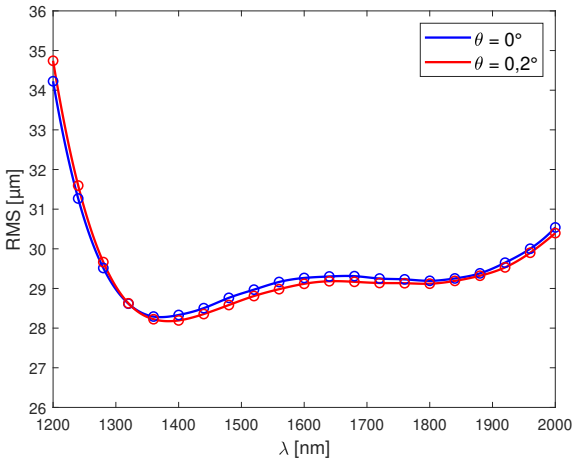

Figure 4: RMS of the flux for each wavelength between 1200 and 2000 nm in the case where the grating is perfectly aligned according to the optical layout and in the case where the grating is misaligned by 0.2° compared to the optical layout.

3.3 PSF's profiles shape, image formation and linearity

For an optical system with a circular entrance aperture, the expected shape of the PSF profiles should be Gaussian. However, due to the off-axis of the system through the mirror and grating, and the properties of the optical elements, the wavefront deforms during the optical path. The shape of the PSF is modified and is no longer Gaussian. Figure 2 clearly shows non-Gaussian PSFs. This disymmetrical shape with a very strong front is typical of off-axis grating spectrometers. Furthermore, the profiles shown in Figure 2 are only represented in a cross-section parallel to the detector. In the direction orthogonal to the detector, the FWHM are much higher. In fact, the overall PSF in the image plane has a shape close to that of an ellipse whose narrowest dimension is the one imaged on the sensor. This elliptical shape is a typical consequence of astigmatism. Thus, in the plane of the linear sensor, the PSF has a dimension of approximately two pixels in the direction parallel to the grating,

while in the other direction the PSF is largely vignetted by the height of one pixel. It could be challenging to improve this design to obtain a spectro-imager given the configuration. Indeed, the PSF is well resolved in only one direction of the image plane.

Moreover, to characterize the image we studied the spectral dispersion on the sensor. The desired configuration is a linear dispersion of the 1200-2000 nm range on the sensor. The method used to analyze dispersion linearity was to plot the position of 21 monochromatic waves on the sensor. A linear regression of these positions as a function of wavelength is used to characterize the dispersion of the spectrum. To assess the quality of the fit, the R^2 parameter was calculated, which represents the fit quality according to the mean square error of the residual and the total mean square error. The optimal fit is indicated by an R^2 value of 1. For the linear regression R^2 was equal to 0.9992, which shows that the dispersion is highly linear. In fact, the optimal fit is achieved with a third-degree polynomial.

All of these studies show that the spectrometer meet the optical requirements for the Uvsq-Sat NG mission and also provide its limitations for further improvements. However, the optical requirements are fulfilled thanks to a narrow entrance slit, the next issue is to determine if the entrance slit's size enable to meet the radiometric requirements.

4. RADIOMETRIC PERFORMANCES OF THE SPECTROMETER

Now that the previous section has validated the instrument's optical performances, we need to determine whether its radiometric performances will be sufficient for CO_2 and CH_4 measurements. Indeed, the entrance slit is sufficiently closed to obtain a spectral resolution of less than 6 nm. However, we need to determine whether, given the slit aperture, the arrangement of the optical elements, the characteristics of the detector and typical irradiances at the TOA, it is possible to obtain an SNR around 2000 above any daylight observation scene.

4.1 Signal Determination

First of all, to asses the radiometric performances of the spectrometer, the method needs to characterize the capability of the instrument to collect the light. The objective is to determine from a spectral irradiance at the TOA what quantity of flux is detected by the sensor. The etendue characterizes how the light spread into the optical system. Equation 5 defines the etendue between the optical aperture (the entrance telescope with a 50 mm diameter) and the entrance slit. The height of the entrance slit h is 300 µm and the width w is 50 µm. The analyzes show that a part of the light propagating through the slit is vignetted by the pixel's size in one direction, the direction of the slit's height. The reciprocal image of the pixel in the plane of the slit h_{eq} depends on the size of the pixel a_{pix} and the magnification γ_λ of the optical system in the direction in which the light is vignetted.

$$G_\lambda = \frac{S_{ap} \times w \times \frac{a_{pix}}{\gamma_\lambda}}{f'^2} \tag{5}$$

where G_λ is the spectral etendue (m^2sr), S_{ap} is the surface of the entrance aperture (m^2), w is the width of the entrance slit (m), a_{pix} is the pixel size in the perpendicular direction of dispersion (m), γ_λ is the magnification of the entrance slit on the sensor on the same direction as a_{pix} and f' is the focal distance of the entrance telescope (m).

To determine the relationship between the entrance irradiance and the flux detected by the sensor, first one considers a spatially and spectrally uniform entrance irradiance. In this case, the measured electron flow is represented by Equation 6.

$$N_{e^-}(\lambda, \tau) = \frac{1}{n_{pix}} \times I_\lambda(\lambda) \times G(\lambda) \times \Delta\lambda \times T_{tot}(\lambda) \times S(\lambda) \times \tau \tag{6}$$

where N_{e^-} is the electron flux received by one pixel according to the number of pixels n_{pix}, the entrance irrandiance I_λ ($Wm^{-2}sr^{-1}nm^{-1}$), the etendue G (m^2sr), the spectral range $\Delta\lambda$ (nm), T_{tot} the total transmission

of the optical system, S the sensor's sensitivity ($e^{-}J^{-1}$) and τ the integration time (s). The total transmission of the optical system is calculated from the transmission of each optical element as described below:

$$T_{tot}(\lambda) = T_{CaF_2}(\lambda) \times T_{Infrasil}(\lambda) \times R_{grating}(\lambda) \times R^2_{mirror}(\lambda)$$

where T_{tot} is the total transmission of the optical system, T_{CaF_2} is the transmission of the CaF_2 glass, $T_{Infrasil}$ is the transmission of the Infrasil glass, $R_{grating}$ is the grating's efficiency and R_{mirror} is the reflectance of the mirror, which has a gold coating.

To estimate the electron flux measured by the instrument, it is necessary to simulate the typical irradiance at the entrance of the instrument at the TOA. The IRIS simulator was designed to manage spectral irradiance at the TOA according to different observation parameters such as the observation scene, the aerosols in the atmosphere or the Solar Zenithal Angle (SZA) (6). This simulator is based on the Second Simulation of Satellite Signal in the Solar Spectrum Vector (6SV) radiative transfer model (7). Figure 5 was made with the IRIS simulator for a typical observation case. In this case, the satellite has a nadir pointing measuring GHG above a pine forest scene. The SZA is supposed to be 20°. From this input spectra and the Equation 6, it was possible to idenify the number of electrons detected by the sensor. The saturation represented on the figure is due to the full-well capacity of the sensor, which is 17.5 Me^{-1}. The integration times were optimally selected, as the sensor did not reach saturation. For a 200 ms integration time, the signal is obviously better than with a 16 µs integration time, however a long integration time can cause blur during measurement. For an instrument moving at a speed of around 6 $km.s^{-1}$ in orbit, this could degrade spatial resolution. The integration time must be optimized to ensure sufficient flux without degrading spatial resolution.

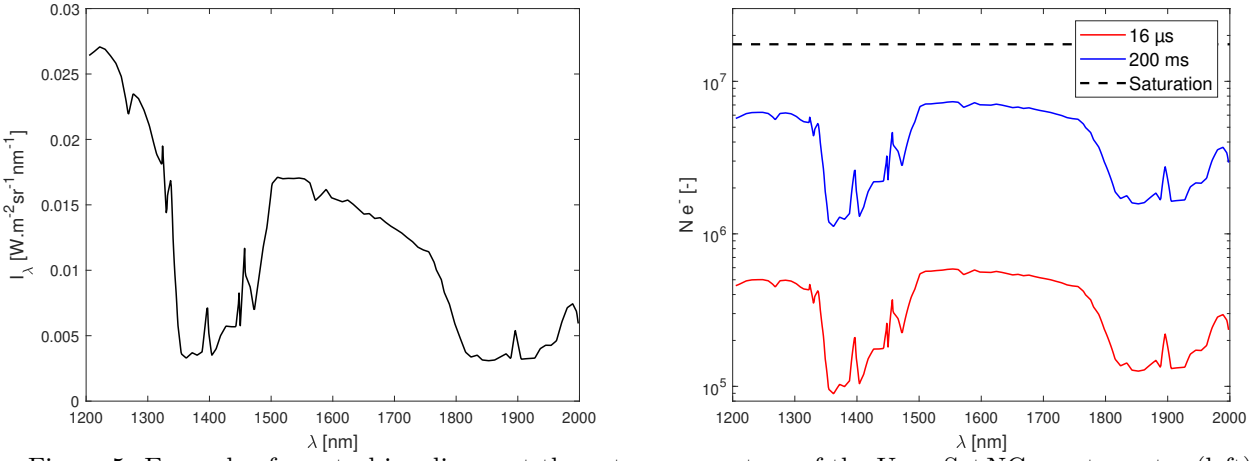

Figure 5: Example of spectral irradiance at the entrance aperture of the Uvsq-Sat NG spectrometer (left). Number of electrons detected by the sensor for integration times of 16 µs and 200 ms (right).

4.2 Noise Determination

The radiometric criterion for validating the Uvsq-Sat NG spectrometer's performances is the SNR. For a 6 nm resolution spectrometer, the SNR must be around 500 to measure CO_2 and CH_4 with the desired accuracy. Equation 6 enables to calculate the signal, here we are estimating the noise during measurements according to multiple variables like the signal measured, the sensor's characteristics and the measurements conditions. Measurement noise is defined as the quadratic sum of different noises. The contributions of the different types of noise are defined below:

- Reading Noise $\mathcal{N}_{RN}$: The reading noise is due to the sensor's characteristics. It is independent of incident flux or integration time. The reading noise of the sensor chosen for the spectrometer is 3125 e^{-}. The estimate of the dark current noise and the electron noise show that this type of noise is negligible.

- Dark Current Noise $\mathcal{N}_{DC}$: The dark current is the current measured by the sensor in the absence of incident flux. This noise is highly dependent on the measurement conditions, in particular the temperature. The chosen InGaAs sensor is cooled to limit the effects of dark current variations on the measurement. Under these observation conditions, the typical dark current is ±4.0 pA. The noise related to the dark current is calculated using the following formula:

$$\mathcal{N}_{DC}(T,\tau) = \sqrt{\frac{I_{DC}(T)}{e} \times \tau}$$

  where $\mathcal{N}_{DC}$ is the dark current noise, I_{DC} is the dark current (A) at a temperature T (K), e is the charge of an electron (C) and τ the integration time of the sensor (s).

- Electron noise $\mathcal{N}_{e^-}$: Electron noise is directly related to the measured signal. It reflects fluctuations in the flux incident on the sensor. The probability of the sensor detecting an incident photon follows a Poisson probability law.

$$\mathcal{N}_{e^-}(\lambda,\tau) = \sqrt{N_{e^-}(\lambda,\tau)}$$

  Where $\mathcal{N}_{e^-}$ is the electron noise, N_{e^-} is the electron flux received by the sensor.

- Additional noise η: This noise represents all noise contributions not previously enumerated. It is presumed to be negligible in comparison to the noise described above.

Global noise $\mathcal{N}$ is defined in Equation 7.

$$\mathcal{N}(\lambda,T,\tau) = \sqrt{\mathcal{N}_{RN}^2 + \mathcal{N}_{DC}^2(T,\tau) + \mathcal{N}_{e^-}^2(\lambda,\tau) + \eta^2} \tag{7}$$

4.3 Signal to Noise Ratio and Sensor's Saturation

SNR calculation is an indicator of radiometric quality. It reflects the system's ability to detect information in relation to measurement noise. A high SNR makes the information intelligible. Equation 8 is calculated from the signal determined Equation 6 and the noise calculated in Equation 7.

$$SNR(\lambda,\tau,T) = \frac{N_{e^-}(\lambda,\tau)}{\mathcal{N}(\lambda,\tau,T)} \tag{8}$$

The SNR measured at the TOA is highly dependent on the spectral irradiance incident at the instrument entrance. The spectrometer must be able to observe the GHGs for as many observation scenes as possible. To assess the instrument's performance for the various scenes that could be observed in orbit, it is necessary to model the radiative transfers in the atmosphere for different observation conditions. For example, irradiance at the TOA is lower at higher zenith solar angles. Similarly, the solar flux reflected at ground level depends on the surface. Oceans reflect less solar flux, while flux reflected by snow can blind space-based instruments. Equation 9 provides the maximum SNR that could be reached for a given integration time when the incident electron flux on the sensor is superior to the sensor's full-well capacity.

$$SNR_{sat}(\tau,T) = \frac{Q_{max}}{\mathcal{N}(\tau,T)} \tag{9}$$

where Q_{max} is the full-well capacity of the sensor.

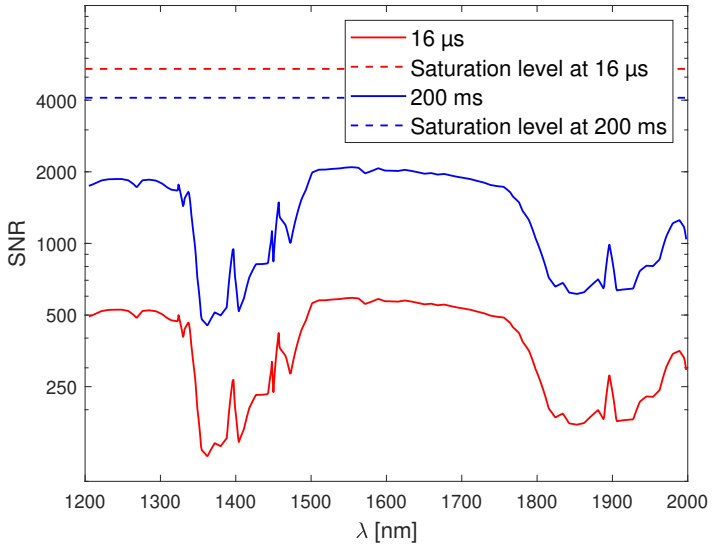

Figure 6: Spectral SNR for integration times of 16 µs and 200 ms and the saturation levels related to this two integration times.

To assess the spectrometer's performance above any daylight scene, IRIS simulation tool provides the spectral irradiances at TOA for various observation cases. This tool enables to simulate radiative transfers at TOA for various conditions (observation surfaces, atmospheric conditions, solar parameters...). Figure 6 provides the spectral SNR measured by the instrument for different integration times. The observed scene is the one of Figure 5, i.e. a pine forest scene with continental aerosols and a SZA of 20°. For an integration time of 16 µs, the SNR just meets the radiometric requirements. With an integration time of 200 ms, the SNR reaches approximately 2000 without exceeding the saturation level. The miniaturized spectrometer appears to fulfill the technical requirement to monitor GHG at TOA.

All the numerical simulations analyzed here assess the spectrometer performances. These performances will have to be confirmed on orbit in 2025 with Uvsq-Sat NG, which has onboard a similar grating spectrometer. Figure 7 provides an illustration of Uvsq-Sat NG during its Assembly, Integration and Tests (AIT) phase.

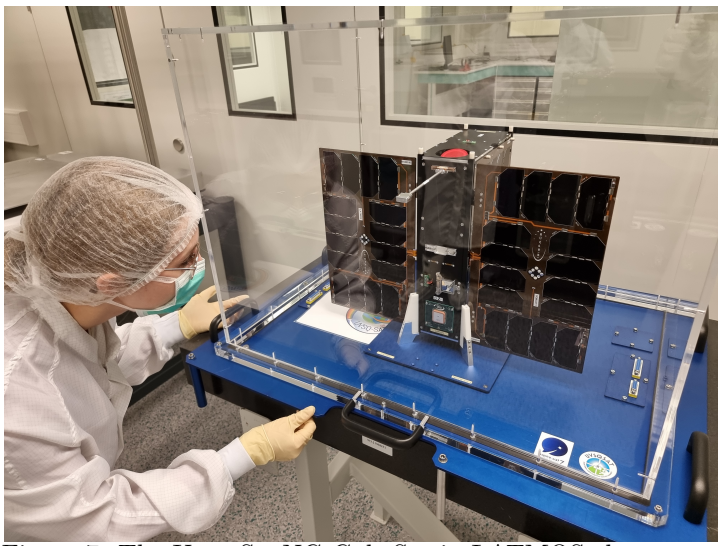
Figure 7: The Uvsq-Sat NG CubeSat in LATMOS cleanroom.

5. PERSPECTIVES AND FUTURE OPTICAL DESIGN

The study of climate will be a crucial aspect of space research in the coming decades. It is imperative that we develop the capacity to monitor GHG concentrations with excellent accuracy and excellent temporal and spatial resolution. This can be achieved through the deployment of a constellation of satellites. Nevertheless, the implementation of a constellation of satellites necessitates the miniaturization of traditional instruments. A multitude of instruments could be subjected to investigation in this regard. For instance, the miniaturization of spectrometers in the thermal infrared region around 8 µm could be studied in order to observe GHG concentrations during both day and nighttime periods, or narrow-band or interferential spectrometers. In the field of broad-band near-infrared spectrometers, in order to accurately measure GHGs, it is necessary to improve the spectral resolution of the instrument. The studies in Sections 3 and 4 evaluate the ability of a spectrometer similar to the one of Uvsq-Sat NG to detect GHG at TOA. Table 3 provides the performances of the Uvsq-Sat NG spectrometer according to the optical and radiometric studies.

Technical performances of the Uvsq-Sat NG spectrometer	
Spectrometer volume	1 Unit ($10\times10\times10$ cm^3)
Spectral resolution	<6 nm on the 1200 - 2000 nm range
SNR @16 µs	<500 on the 1200 - 2000 nm range
Field of view	0.15°
Scientific performances of the Uvsq-Sat NG spectrometer @16 µs	
CO_2 absolute accuracy	~ 3 ppm
CH_4 absolute accuracy	~ 40 ppb
Spatial resolution	1 to 2 km
Temporal resolution	>30 days

Table 3: Expected performances of the Uvsq-Sat NG spectrometer for an integration time of 16 µs.

The Uvsq-Sat NG spectrometer represents a pioneering approach to a novel instrument implementation method for greenhouse gas observation. For an integration times of 16 µs, the spectrometer exhibits encouraging performance, suggesting that further enhancements would enable it to better align with international scientific standards. To improve this first miniaturized instrument, the aim is to design a new spectrometer with a 1 nm resolution. Indeed, Figure 8 provides GHG transmittance at TOA for a 1 nm and a 5 nm spectral resolution, which clearly demonstrates the value of a 1 nm spectrometer. With a 5 nm spectrometer, the instrument will only be able to resolve the absorption bands of the various GHG, while with higher resolution, it will be possible to resolve the absorption lines. This is a relevant perspective to resolve methane narrow absorption line around 1670 nm. However, instrument miniaturization is the main obstacle to improving resolution. The spectrometer presented in the previous sections has a resolution of around 5 nm for a volume of one unit ($10\times10\times10$ cm^3). Increasing spectral resolution by a factor of 5 is a real challenge, and one we're trying to address.

For a grating spectrometer, we need to disperse the entire 1200-2000 nm spectral range on a single sensor. To obtain 1 nm of resolution in this range, the first idea would be to use the same type of configuration as above, but with a larger linear sensor. For an 800 nm range, the focal plan would require at least 1600 pixels. For 50 µm pixels, this means that the sensor would measure at least 80 mm, which is extremely unusual for a linear sensor. Moreover, this sensor's size is too high to get excellent spectral resolution with a short focal instrument. The first idea would be to reduce the pixel's size, however that would mean drastically reducing the entrance slit, which is undesirable given the radiometry. To overcome the problem, we propose to divide the 800 nm range into several bands and image them on a matrix sensor. To achieve this, it is necessary to use an echelle spectrometer.

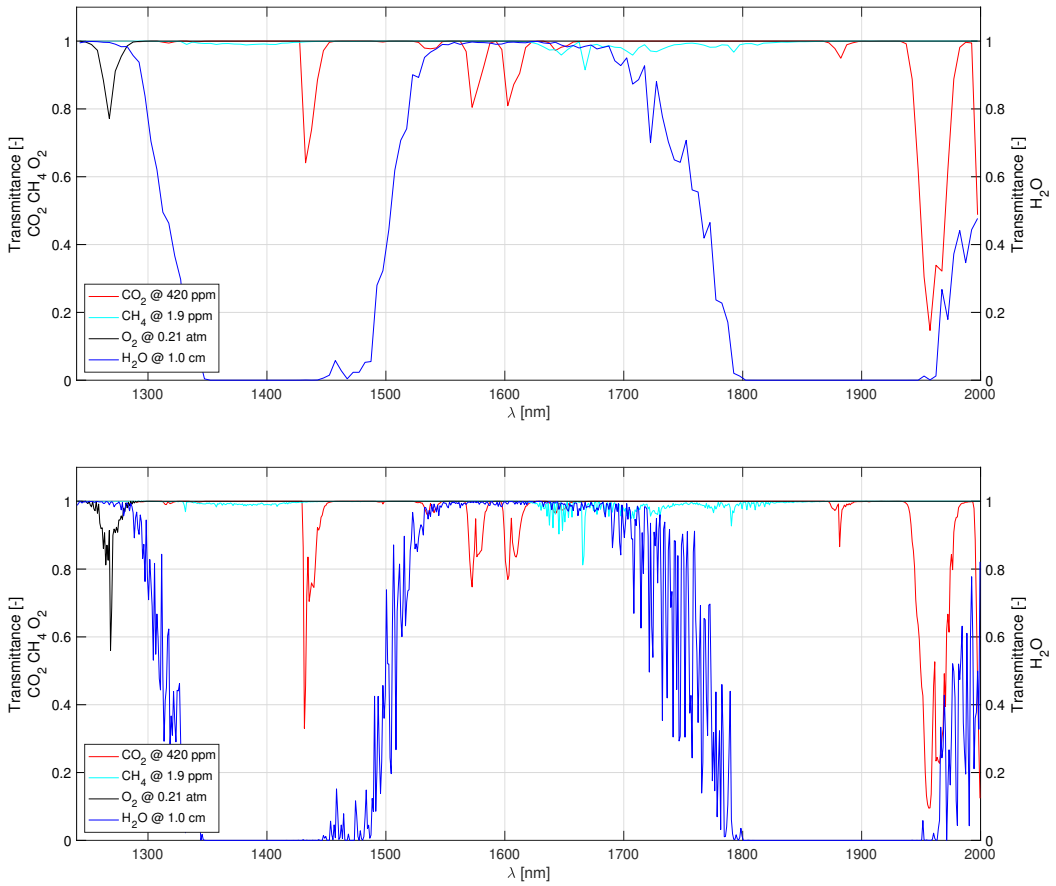

Figure 8: GHG transmittance at a 5 nm (above) and 1 nm resolution (below).

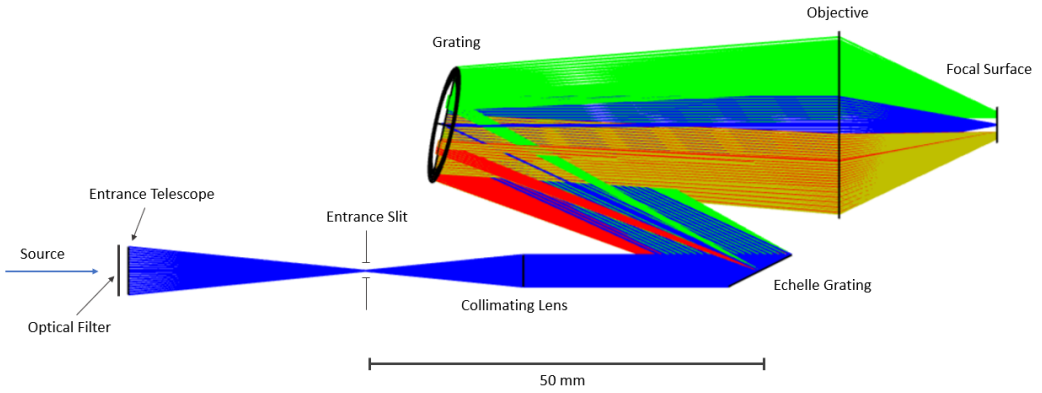

Figure 9: Optical concept for CLARA, a miniaturized 1 nm spectrometer.

Figure 9 illustrates a concept for an echelle spectrometer named CLARA that could be imagined onboard a CubeSat. First, an optical filter is used to select the 1200-2000 nm measurement range to reduce stray light inside the system. This filter can be placed as the first input element, or just after the input telescope to protect it from external radiation. Next, the input telescope focuses the incident flux in the plane of the slit. The slit

plays an important role in spectral resolution and radiometry. In this design, it is assumed to be 50×50 µm, which is a compromise between spectral resolution, spatial resolution and radiometric performances. This type of instrument uses two gratings, the first of which is an echelle grating that disperses light at high diffraction orders (several dozen) to widely disperse the spectrum. However, these diffraction orders are superposed one on top of the other after the first grating, so a second grating must be used to separate the different diffraction orders and image them on a matrix sensor using the objective. This grating is said to be crossed with the first one, with the dispersion plane being orthogonal to that of the echelle grating. This configuration is aimed at spreading the orders of the echelle grating along the other axis of the focal plane. The 1200-2000 nm spectral range is then separate in few spectral ranges on the sensor. Figure 10 shows the principle for image formation on the sensor. Each point represents the paraxial image for one monochromatic wave. For each spectrum on the sensor for a diffraction order, it's possible to reconnect this spectrum with the one of the following diffraction order to find the 1200-2000 nm spectrum. As first result, the displacement of a spot at a wavelength one nanometer higher is about 40 µm. That's mean that the pixel's size of the sensor must be thinner than 20 µm. For this application, the G16564-0808T Hamamatsu sensor could be a good candidate with a pixel's size of 20 µm and the sensor's size of 320×256 pixels. For the global system, we could imagine that a two units' cube (20×10×10 cm^3) will be needed. Table 4 shows the technical requirements for such an echelle spectrometer and its expected scientific measurements accuracy.

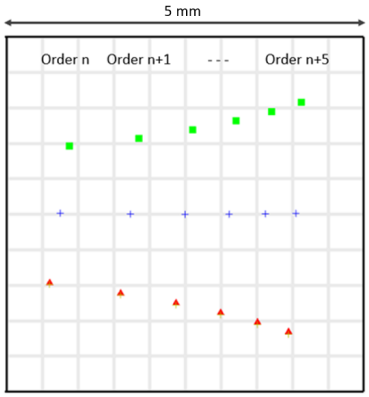

Figure 10: Example of spot diagram on the matrix sensor.

Technical requirements for the CLARA spectrometer	
Spectrometer volume	2 Units (10×10×20 cm^3)
Spectral resolution	1200 - 2000 nm
Spectral resolution	<1 nm
SNR	>500
Sensor	320×256 pixels
Pixels size	20×20 μm^2
Field of view	0.1°
Expected scientific performances for the CLARA spectrometer	
CO_2 absolute accuracy	$\sim$ 1 ppm
CH_4 absolute accuracy	$\sim$ 12 ppb
Spatial resolution	$\sim$ 1 km
Temporal resolution	>30 days

Table 4: Expected performances of the new echelle spectrometer.

The optical design presented in this section is a serious avenue on which we will work on to make a 1 nm resolution spectrometer to accurately monitor GHG and to create a CubeSat constellation for climate. This is a work in progress, the optical design will be ended in the following months to build a prototype and then a flight

model. This is a challenging work opened to international collaboration to develop a satellites constellation to study ECV.

6. CONCLUSIONS

Uvsq-Sat NG will be launched in 2025 to inaugurate a new nanosatellites constellation in order to observe Greenhouse Gas (GHG) in near-real time. The optical and radiometric performances of miniaturized Uvsq-Sat NG spectrometer show that the instrument would be able to measure CO_2 concentrations with ± 3.0 ppm accuracy and CH_4 concentrations with ± 40.0 ppb accuracy for an integration time of 16 µs. Those performances have been determined with optical simulations. Before the launch, a pre-flight calibration campaign will assess and validate the performances of the instrument. The full performances will be validated on orbit in 2025.

At the same time, the LATMOS develops a new instrument to reach a better resolution and improve GHG measurements. This new instrument is based on the optical design of an echelle spectrometer. If this spectrometer can fulfill a 1 nm spectral resolution, it will enables to determine GHG at Top Of Atmosphere (TOA) with high accuracy for a CubeSat payload ($\sim$ 1 ppm for CO_2 and $\sim$ 12 ppb for CH_4). This would enables to resolve the GHG absorption lines and to be more precise in the local sinks and sources determination. The final objective is to fulfill the international spatio-temporal requirements with a satellites constellation. The enhancement of the inventory of international GHG sources will facilitate the more precise identification and quantification of GHG emitters, thereby enabling the implementation of public and taxation policies that are adapted to the fight against anthropogenic gas emissions.

References

[1] Pachauri, R. and (eds.), L. M., "Ipcc, 2014: Climate change 2014: Synthesis report. contribution of working groups i, ii and iii to the fifth assessment report of the intergovernmental panel on climate change.," *IPCC* (2014).

[2] Agreement, P., "Paris agreement," in [*report of the conference of the parties to the United Nations framework convention on climate change (21st session, 2015: Paris). Retrived December*], **4**, 2017, HeinOnline (2015).

[3] Schuur, E. A., McGuire, A. D., Schädel, C., Grosse, G., Harden, J. W., Hayes, D. J., Hugelius, G., Koven, C. D., Kuhry, P., Lawrence, D. M., et al., "Climate change and the permafrost carbon feedback," *Nature* **520**(7546), 171–179 (2015).

[4] Zemp, M., Chao, Q., Han Dolman, A. J., Herold, M., Krug, T., Speich, S., Suda, K., Thorne, P., and Yu, W., "Gcos 2022 implementation plan," *Global Climate Observing System GCOS* (244), 85 (2022).

[5] Meftah, M., Clavier, C., Sarkissian, A., Hauchecorne, A., Bekki, S., Lefèvre, F., Galopeau, P., Dahoo, P.-R., Pazmino, A., Vieau, A.-J., et al., "Uvsq-sat ng, a new cubesat pathfinder for monitoring earth outgoing energy and greenhouse gases," *Remote Sensing* **15**(19), 4876 (2023).

[6] Clavier, C., Meftah, M., Sarkissian, A., Romand, F., Hembise Fanton d'Andon, O., Mangin, A., Bekki, S., Dahoo, P.-R., Galopeau, P., Lefèvre, F., et al., "Assessing greenhouse gas monitoring capabilities using solatmos end-to-end simulator: Application to the uvsq-sat ng mission," *Remote Sensing* **16**(8), 1442 (2024).

[7] Vermote, E. F., Tanré, D., Deuze, J. L., Herman, M., and Morcette, J.-J., "Second simulation of the satellite signal in the solar spectrum, 6s: An overview," *IEEE transactions on geoscience and remote sensing* **35**(3), 675–686 (1997).